Supporting Information

# Continuous Addition Kinetic Elucidation: Catalyst and Reactant Order, Rate Constant, and Poisoning from a Single Experiment

Peter J. H. Williams[a], Charles Killeen[a], Ian C. Chagunda[a], Brett Henderson[a], Sofia Donnecke[a], Wil Munro[a], Jaspreet Sidhu[a], Denaisha Kraft[a], David A. Harrington*[b], J. Scott McIndoe*[a]

[a]Department of Chemistry, University of Victoria, PO Box 1700 STN CSC, Victoria, BC V8W 2Y2, Canada.
Tel: +1 (250) 721-7181; E-mail: mcindoe@uvic.ca.
[b]Department of Chemistry, University of Victoria, PO Box 1700 STN CSC, Victoria, BC V8W 2Y2, Canada.
Tel: +1 (250) 721 7166; E-mail: dharr@uvic.ca.

## Abstract

Kinetic analysis of catalytic reactions is a powerful tool for mechanistic elucidation but is often challenging to perform, limiting understanding and therefore development of these reactions. Establishing order in a catalyst is usually achieved by running several reactions at different loadings, which is both time-consuming and complicated by the challenge of maintaining consistent run-to-run experimental conditions. **C**ontinuous **A**ddition **K**inetic **E**lucidation (CAKE) was developed to circumvent these issues by continuously injecting catalyst into a reaction while monitoring reaction progress over time. For reactions that are *m*th order in a single yield-limiting reactant and *n*th order in catalyst, a plot of reactant concentration against time has a shape dependent only on the orders *m* and *n*. Therefore, fitting experimental CAKE data (using open access code or a convenient web tool) allows the reactant and catalyst orders, rate constant, and the amount of complete catalyst inhibition to be determined from a single experiment. Kinetic information obtained from CAKE experiments showed good agreement with literature.

**DOI: 00.0000/xxxxxxxxxx**

## Table of Contents

## Materials and Methods

All solvents were purchased from Fisher Scientific and used without further purification, unless otherwise specified.

Hydrogen peroxide (30%, non-stabilized, Fisher Scientific), potassium iodide (reagent grade, Caledon), potassium bromide (ACS reagent grade, Caledon), L-ascorbic acid (ACS reagent grade, ACP), sulfuric acid (98%, ACS reagent grade, Fisher Scientific), sodium carbonate (>99.5%, ACS, Bio Basic Inc. Canada), silver nitrate (ACS reagent grade, ECP), 4-methoxybenzeneboronic acid (98%, Oakwood), tetrakis(triphenylphosphine)palladium(0) (99%, Sigma Aldrich), ethanol (anhydrous, Greenfield Global), beta-nicotinamide adenine dinucleotide (97%, Fisher Scientific), 2-amino-2-hydroxymethyl-propane-1,3-diol (TRIS, ultra-pure grade, Bio Basic Inc. Canada) and alcohol dehydrogenase (from *Saccharomyces cerevisiae,* 300 u $mg^{-1}$ protein, Millipore Sigma) were used without further purification.

For the Suzuki coupling reaction, methanol (HPLC grade) was distilled from calcium hydride before use. Gases were purchased from Airgas (Calgary, Canada) and used without further purification.

UV-Vis spectra were collected using an ASEQ Instruments LR-1 compact spectrometer (version 2.1, Configuration B) equipped with a reflection fiber optic Y-cable probe (F01_R03) fitted with a Teflon transflectance dip probe (LQ_R01) and a D2-S1 deuterium/halogen light source. The spectral range of the LR-1 is 200-1200 nm with a resolution of <2 nm. The deuterium light source was used for all experiments and all spectra recorded between 200-500 nm with 10 point boxcar averaging. Spectra were obtained each second by averaging over 10 spectra, each with a scan time of 100 ms. For this, the fiber optic probe was clamped such that its outlet and the transflectance dip probe were immersed in the centre of a solution and the set-up wrapped in aluminum foil to prevent external light disturbances during experiments. Prior to experiments, a reference spectrum was recorded in $H_2O$, allowing absorbance spectra to be recorded.

Mass spectra were collected by a Waters (Milford, USA) Synapt G2-S*i* mass spectrometer and analyzed using Waters MassLynx V4.2. The Synapt G2-S*i* was operated in positive ion resolution mode. The capillary voltage was held at 3.0 kV, with the desolvation settings optimized with source temperature 70 °C, desolvation temperature 180 °C, desolvation gas flow rate 50 L $h^{-1}$, and cone gas flow 400 L $h^{-1}$. The mass range was set to *m/z* 100-600 with scan durations of 1 s.

## Experimental Procedures

### $O_2$ evolution from KI-catalyzed $H_2O_2$ decomposition

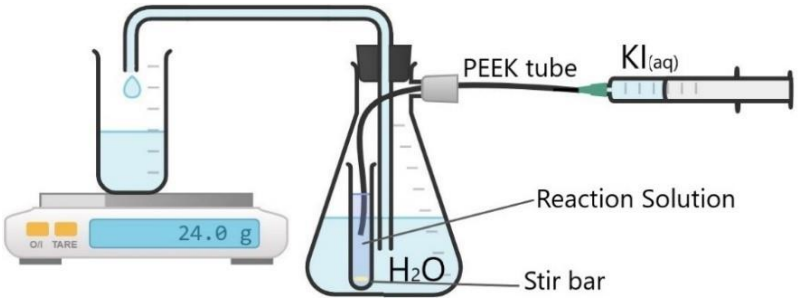


**Fig. SI1** Experimental set-up for $O_2$ evolution CAKE reaction.

*General*

$$H_2O_2 \xrightarrow[\text{Additive(s)}]{\text{Catalyst(s)}} H_2O + ½\ O_2$$

The experiment was adapted from literature procedures[25,26] and performed using the set-up shown in Fig. SI1. $H_2O_2$ solution (0.400 M in $H_2O$, 10 mL, 4.00 mmol, 1.00 eq.) was placed in a test tube equipped with a stirrer bar and, if required, poison deliberately added. The test tube was placed inside a Buchner flask (250 mL) containing $H_2O$ (~100 mL). The Buchner flask outlet was sealed using a septum and parafilm. Pre-loaded PEEK tubes attached to syringes containing catalyst solution were inserted through the septum and into the centre of the reaction solution. Hot glue was applied to the exterior of the septum to seal around PEEK tubing. The Buchner flask inlet was sealed with a rubber stopper and parafilm. The rubber stopper was equipped with a rigid transparent plastic tube, such that the plastic tube reached the base of the $H_2O$ in the Buchner flask. Air was injected through the septum to fill the plastic tube with $H_2O$ and then removed. Once pressure equalised, the plastic tube outlet was placed over a beaker on a mass balance. Mass of $H_2O$, and hence volume of $O_2$ produced, was recorded using a photographic timelapse of the mass balance display (12 frames $min^{-1}$). The reaction solution was stirred for 2.0 min before addition of catalyst solution(s). All reactions effervesced during the reaction, following catalyst addition. The reaction was stopped after product formation had ended. Upon reaction completion, [$O_2$] was assumed constant. Data were processed to account for evaporation of expelled $H_2O$. Only data points with a significant mass difference compared to the previous data point were extrapolated. Although this reaction is robust, the simple experimental apparatus used was at risk of gas leakage. Although ~100% gas yields were frequently observed, up to 10% leakage was observed in some experiments. To circumvent this leakage, product moles were scaled such that final product moles were equivalent to 100% yield for CAKE fitting, with the resulting fit being rescaled accordingly for presentation of results. For CAKE fitting, all $O_2$ was assumed to remain in solution, i.e., moles of $O_2$ in solution were assumed equal to moles of $O_2$ gas produced experimentally.

*CAKE KI experiment*

$$H_2O_2 \xrightarrow[H_2O]{KI\ (0.005\ eq.\ min^{-1})} H_2O + ½\ O_2$$

The general reaction procedure was followed as described above, with continuous addition of KI solution (5.00 M in $H_2O$, 4.00 µL $min^{-1}$, 20.0 µmol $min^{-1}$, 0.005 eq. $min^{-1}$) using a syringe pump.

*Non-CAKE KI experiment*

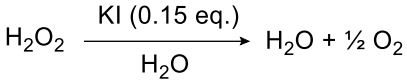


The general reaction procedure was followed as described above, with a single addition of KI solution (5.00 M in $H_2O$, 120 µL, 600 µmol, 0.15 eq.).

*CAKE KBr experiment*

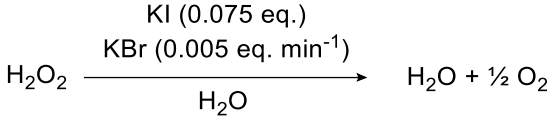


The general reaction procedure was followed as described above, with a single addition of KI solution (5.00 M in $H_2O$, 60 µL, 300 µmol, 0.075 eq.) and continuous addition of KBr solution (2.50 M in $H_2O$, 8.00 µL $min^{-1}$, 10.0 µmol $min^{-1}$, 0.005 eq. $min^{-1}$) using a syringe pump.

*CAKE poisoning experiment*

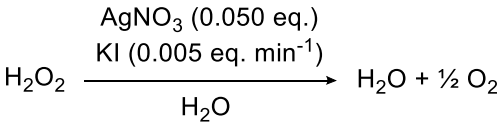


The general reaction procedure was followed as described above, with $AgNO_3$ (34.0 mg, 200 µmol, 0.050 eq.) poison added into the $H_2O_2$ solution and KI solution (5.00 M in $H_2O$, 4.00 µL $min^{-1}$, 20.0 µmol $min^{-1}$, 0.005 eq. $min^{-1}$) continuously added using a syringe pump. A yellow precipitate formed during the experiment.

**Ascorbic acid oxidation**

*General*

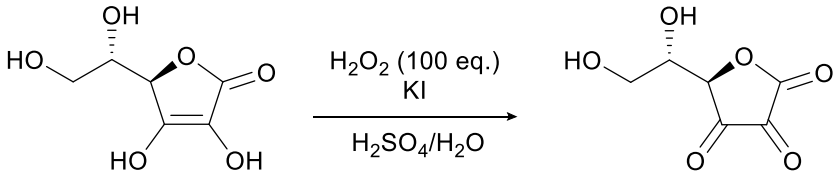


L-ascorbic acid L-dehydroascorbic acid

The experiment was adapted from literature procedures.[38–40] $H_2O_2$ (100 mM in $H_2O$, 1.00 mL, 100 µmol, 100 eq.), L-ascorbic acid (10.0 mM in $H_2O$, 100 µL, 1.0 µmol, 1.0 eq.), $H_2SO_4$ (100 mM in $H_2O$, 1.00 mL, 100 µmol, 100 eq.) and $H_2O$ (2.90 mL) were placed in a flask equipped with a stirrer bar. The UV-Vis immersion probe and pre-loaded PEEK tubing attached to a syringe containing KI solution were then placed in the flask and the set-up covered with aluminium foil. The reaction solution was stirred for 1.0 min before the addition of KI solution. Data were processed by integrating absorbance between 260-270 nm. Ascorbic acid concentration was assumed to be zero after the minimum integrated absorbance was reached.

*CAKE experiment*

The general reaction procedure was followed as described above, with continuous addition of KI solution (200 mM in $H_2O$, 5.00 µL $min^{-1}$, 1.00 µmol $min^{-1}$, 1.0 eq. $min^{-1}$) using a syringe pump.

*Non-CAKE experiment*

The general reaction procedure was followed as described above, with a single addition of KI solution (200 mM in $H_2O$, 35 µL, 7.0 µmol, 7.0 eq.).

**Suzuki coupling**

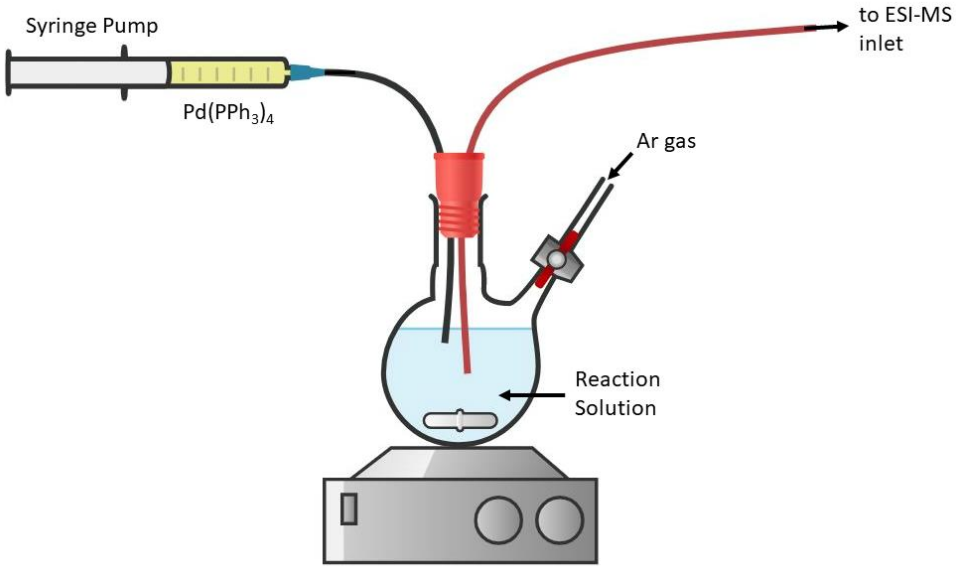


**Fig. SI2** Experimental set-up for Suzuki Coupling CAKE reaction.

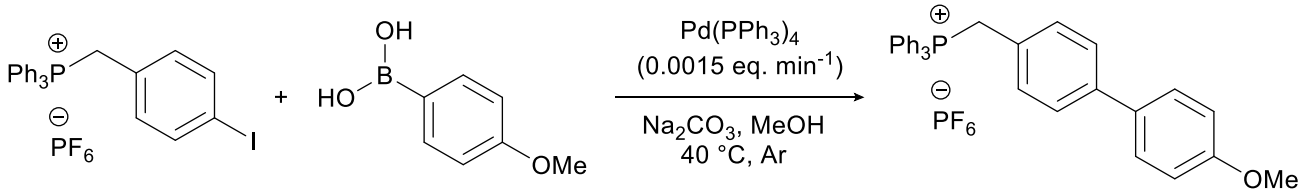


The reaction was monitored using PSI-ESI-MS techniques[41] using the set-up shown in Fig. SI2. The experiment was set-up and performed under an argon atmosphere using standard Schlenk and glovebox techniques. Charged aryl iodide $[Ph_3PCH_2C_6H_4I]^+[PF_6]^-$ was synthesized according to a literature procedure and consistent characterization data obtained.[42] $Na_2CO_3$ (2.0 mg, 9.4 µmol, 30 eq.) and MeOH (30 mL) were placed in a Schlenk flask equipped with a stirrer bar and heated to 40 °C. The charged aryl iodide $[Ph_3PCH_2C_6H_4I]^+[PF_6]^-$ (1.5 mM in MeOH, 0.2 mL, 0.30 µmol, 1.0 eq.) and 4-methoxyphenylboronic acid (2.0 mM in MeOH, 1.0 mL, 2.0 µmol, 6.7 eq.), were injected into the flask through the septum, using a syringe. The reaction mixture was monitored by ESI-MS at an injection rate of 31 µL $min^{-1}$ until equilibrium was reached and a steady signal intensity was achieved. Pre-loaded PEEK tubing attached to a syringe containing $Pd(PPh_3)_4$ precatalyst solution (0.10 mM in degassed tetrahydrofuran) was inserted through the septum and into the centre of the reaction solution. ESI-MS spectra were recorded for 1.0 min before $Pd(PPh_3)_4$ precatalyst solution was added using a syringe pump (30 µL $min^{-1}$, 3.0 nmol $min^{-1}$, $1.5\times10^{-3}$ eq. $min^{-1}$). The reaction was stopped after reactant consumption and product formation had ended (~18 min).

### Ethanol oxidation catalyzed by alcohol dehydrogenase (ADH) enzyme

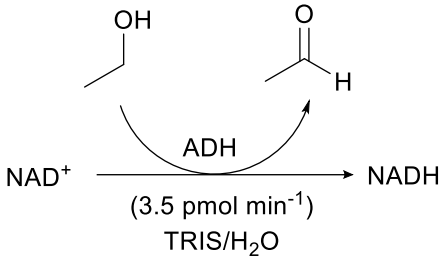


The experiment was adapted from literature procedures.[37,43,44] Ethanol (1.00 M in $H_2O$, 1000 µL, 1.00 mmol, 100 eq.), nicotinamide diadenine nucleotide ($NAD^+$) (10.0 mM in $H_2O$, 1000 µL, 10.0 µmol, 1.0 eq.), tris(hydroxymethyl)aminomethane (TRIS) buffer (200 mM in $H_2O$, pH 9.0, 400 µL), and $H_2O$ (1600 µL) were placed in a flask equipped with a stirrer bar. ($\lambda_{max}$ of NADH = 340 nm). The UV-Vis immersion probe and pre-filled PEEK tubing attached to a syringe containing alcohol dehydrogenase (ADH) solution (0.7 µM in 20 mM TRIS buffer) were then placed in the flask and the set-up covered with aluminium foil. The reaction solution was stirred for 1.0 min before the ADH solution was continually injected (5.00 µL $min^{-1}$, 3.5 pmol $min^{-1}$, $3.5\times10^{-7}$ eq. $min^{-1}$) using a syringe pump. The reaction was stopped once NADH formation had ended (~8.6 min). Data were processed by integrating absorbance between 330-350 nm.

### Fitting parameters

For all fittings, an initial estimate for k was determined from experimental $t_{1/2}$. Additionally, reactant order and catalyst order were fitted between 0-2. All reactions fitted to the product were assumed to achieve 100% yield (i.e., final product concentration was proportional to initial reactant concentration, accounting for stoichiometries). Neither experimental smoothing nor decreasing of stepsize for solving the differential equation were performed. All other parameters required to use CAKE fitting are given in the descriptions of each experiment or Table SI1.

**Table SI1** Fitting parameters used for fitting data during processing of different kinetic experiments.

| Reaction | Processed data file number | $t_{pois}$ bound | Scale average fit | Fit aspect |
|---|---|---|---|---|
| $O_2$ evolution | 1 | fixed | 1 | p |
| KBr $O_2$ evolution | 2 | fixed | 1 | p |
| Ascorbic acid oxidation | 3 | fixed | 30 | r |
| Poisoned $O_2$ evolution | 4 | variable | 1 | p |
| Ascorbic acid oxidation | 5 | variable | 30 | r |
| Suzuki coupling | 6 | variable | 10 | r+p |
| Enzymatic catalysis | 7 | variable | 60 | p |

## Results and Discussion

### Guidance on catalyst addition rate

If a reliable system for monitoring a non-CAKE reaction has been pre-established, its half-life ($t_k$) would typically be a suitable half-life for the corresponding CAKE system ($t_{1/2}$). Therefore, setting $t_{1/2}$ and $t_k$ as equal, allows Eq. (5) to be arranged as:

$$t_{\mathrm{p}} = \frac{t_{\mathrm{k}}}{(n+1)^{1/n}}$$

Catalyst orders of 0.01, 1 and 2 lead to $t_p = 0.37t_k$, $0.5t_k$ and $0.58t_k$ respectively. A zero order "catalyst" ($n = 0$) has no solution, as its rate of addition does not affect the rate of reaction. Therefore, if catalyst order is unknown, performing catalyst addition at a rate such that $t_p = 0.5t_k$ is typically suitable. For example, if the non-CAKE catalyst concentration is 1 mM and half-life ($t_k$) is 10 min, then a suitable $t_p$ = 5 min and hence rate of catalyst addition ($p$) = 0.2 mM min$^{-1}$.

**Computational aspects**

From a computational point of view, numerical solution of the differential equation within each iteration of the least-squares fitting routine offers the ultimate in flexibility for adding effects such as correction for volume increase, which may not have an exact analytical solution. This increases the computational effort required, and potentially introduces a numerical error. However, comparisons with fitting directly to the analytical equations showed similar results, well within the parameter error estimates, even for the simplest (Euler) method for solving the differential equation, provided there were a reasonable number of data points. Improved results for smaller data sets could be achieved by decreasing the stepsize for solving the differential equation to a fraction of the data point interval, or by using a higher order solver, e.g., fourth order Runge-Kutta.

Numerical solution also has the advantage of not having to choose between the two forms of Eq. (3) in the paper. If the order in reactant is completely unknown, a single piecewise function having both forms may be used. In practice, the piecewise function worked well when using the first-order formula for $m$ in the range $0.95 < m < 1.05$, and the $m \neq 1$ formula otherwise.

As usual in non-linear least-squares fitting, convergence to the correct minimum requires initial estimates for the parameters and/or ranges in which they occur. The reaction orders are in a small range, say 0-3, and fitting was found to be successful with an initial estimate in this range. The rate constants, however, may vary over orders of magnitude, and required an estimate in the correct order of magnitude. An effective way to solve this problem is to use an estimate of $t_{1/2}$, easily found from the experimental data, and combine it with the known $p$ and estimates of $m$ and $n$ to calculate an initial value of $k$ using the formula for $t_{1/2}$ given in the mathematical derivations section of the SI, Eq. (40).

**Computational simulations**

*Fits for m = 0, 1, 2 and n = 0, 1, 2*

Fitted simulated data with normally-distributed added noise of 5% standard deviation for integer orders 0, 1 and 2 is shown in Fig. SI3. The average standard error for the fitted orders was 0.04 with worst case 0.17, and for the rate constants was 8% with worst case 14%. That is, despite the very similar shapes in some cases, the orders and rate constants can be reliably extracted.

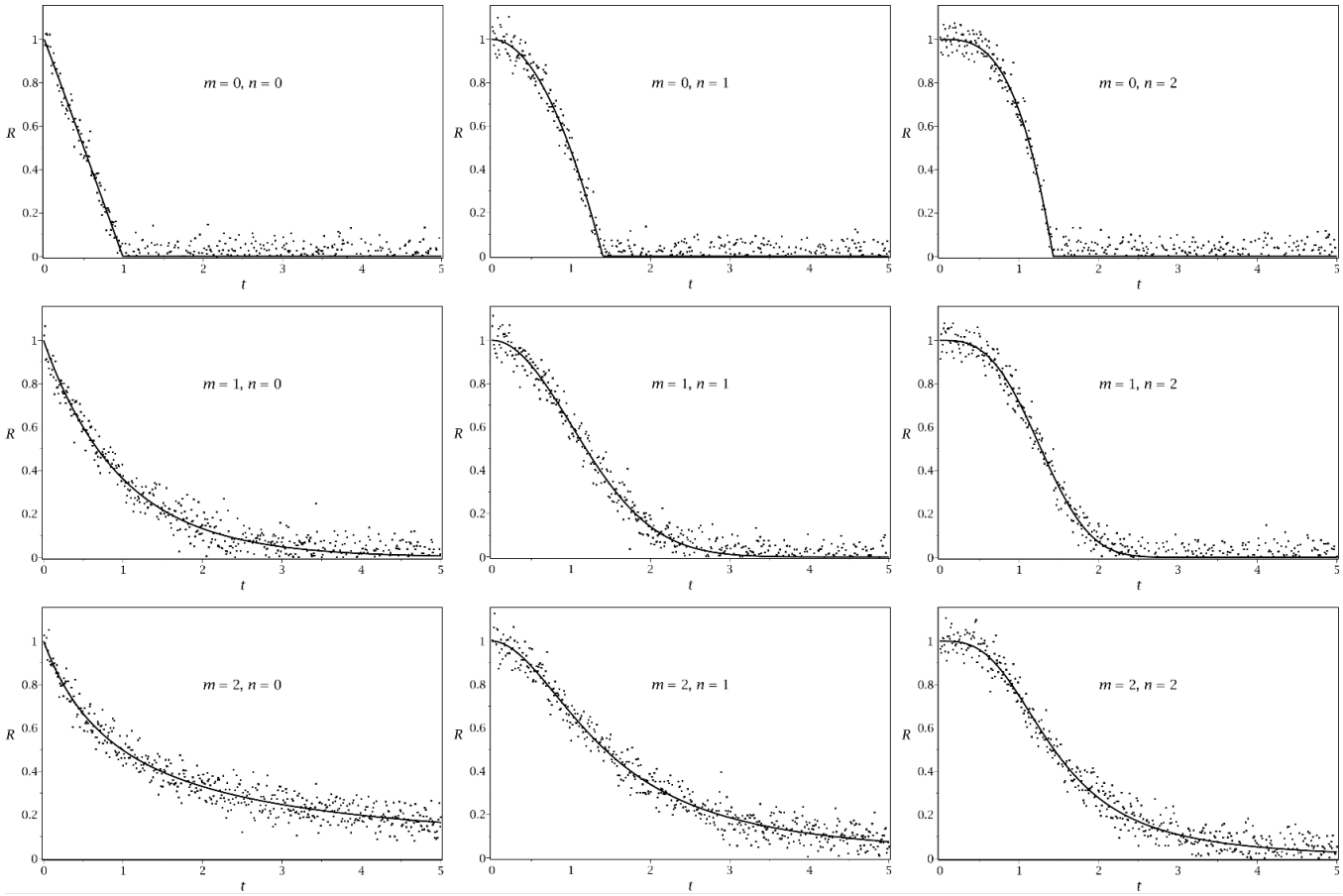


**Fig. SI3** Simulated data for the 9 cases of *m* and *n* for integer values of 0, 1 and 2.

Concentration vs time profiles were generated by and fitted to the equations for $m = 0$, $m = 1$ and general $m$ (used for $m = 2$):

$$R0n := \begin{cases} R_0 \left| 1 - \dfrac{k p^n t^{n+1}}{(n+1)\, R_0} \right| & t < \left( \dfrac{R_0 (n+1)}{k p^n} \right)^{\frac{1}{n+1}} \\ 0 & otherwise \end{cases}$$

$$R1n := R_0 \, e^{-\frac{k p^n t^{n+1}}{n+1}}$$

$$Rmn := R_0 \left| \frac{(m-1)\, k p^n t^{n+1}}{(n+1)\, R_0^{-m+1}} + 1 \right|^{-\frac{1}{m-1}}$$

Fixed parameters were $R_0 = 1$ and $p = 1$. Data (500 points) were generated with these and $k = 1$ and the stated $m$ and $n$ values. Fitted parameters were $k$ and $n$, and also $m$ for the data generated with $m = 2$. The generated data had random normally-distributed noise with a standard deviation of 0.05 added. The implementation was using Maple 2015, with fitting by Maple's NLPSolve routine using the nonlinearsimplex method.

Fitted values are given in Table SI2, given as the fitted value ± standard error.

**Table SI2** Fitted values and standard errors shown for each value of *m*, *k*, and *n*.

| | | $n$ = 0 | $n$ = 1 | $n$ = 2 |
|---|---|---|---|---|
| $m$ | 0 | $k = 1.02 \pm 0.04$<br>$n = 0.01 \pm 0.03$ | $k = 1.02 \pm 0.02$<br>$n = 0.97 \pm 0.05$ | $k = 1.02 \pm 0.01$<br>$n = 2.11 \pm 0.08$ |
| | 1 | $k = 1.00 \pm 0.02$<br>$n = -0.01 \pm 0.02$ | $k = 0.98 \pm 0.01$<br>$n = 0.99 \pm 0.04$ | $k = 1.00 \pm 0.02$<br>$n = 1.98 \pm 0.06$ |
| | 2 | $k = 1.04 \pm 0.14$<br>$n = 0.02 \pm 0.06$<br>$m = 2.03 \pm 0.17$ | $k = 0.94 \pm 0.06$<br>$n = 0.92 \pm 0.09$<br>$m = 1.92 \pm 0.11$ | $k = 1.05 \pm 0.06$<br>$n = 2.07 \pm 0.15$<br>$m = 2.14 \pm 0.12$ |

*Simulations with varying rate constants and injection speeds*

We used simulations to probe the limits of the method when the experimental and kinetic timescales are significantly mismatched. The case $m = n = 1$ was investigated in detail, taking for simplicity $C_{ref} = R_0 = 1$ M, with the results summarized in Table SI3. Details of the fitting method are given in the Table caption.

**Table SI3** Fixed parameters were $R_0 = 1$ and $m = 1$. Data (500 points) were generated with these and $n = 1$ and the stated $p$ and $k$ values over the time $t_{max}$. This is the time to add the number of equivalents of catalyst given in parentheses. Fitted parameters were $k$ and $n$. If the concentration unit is M and time unit is min, then $p$ is in M min$^{-1}$ and $k$ is in M$^{-1}$ min$^{-1}$. The generated data had random normally-distributed noise with a standard deviation of 0.05 added. The implementation was using Maple 2015, with fitting by Maple's NLPSolve routine using the nonlinearsimplex method. Fitted values are given as the fitted value ± standard error.

| Fig. | $p$ | $k$ | $t_{max}$ (equiv) | $n$ (fitted) | $k$ (fitted) |
|---|---|---|---|---|---|
| (a) | 1 | 1 | 5 (5) | $0.93 \pm 0.03$ | $0.97 \pm 0.01$ |
| (b) | 1 | $10^{-2}$ | 5 (5) | $1.04 \pm 0.21$ | $(1.01 \pm 0.20) \times 10^{-2}$ |
| (c) | 1 | $10^{2}$ | 5 (5) | $0.93 \pm 0.11$ | $(0.82 \pm 0.21) \times 10^{2}$ |
| | 1 | $10^{-2}$ | 30 (30) | $0.98 \pm 0.03$ | $(1.05 \pm 0.06) \times 10^{-2}$ |
| | $10^{-2}$ | $10^{-2}$ | 100 (1) | $0.95 \pm 0.06$ | $(0.95 \pm 0.05) \times 10^{-2}$ |
| | 1 | $10^{2}$ | 0.5 (0.5) | $0.95 \pm 0.03$ | $(0.88 \pm 0.07) \times 10^{2}$ |
| | $10^{2}$ | $10^{2}$ | 0.05 (5) | $1.06 \pm 0.04$ | $(1.00 \pm 0.01) \times 10^{2}$ |
| | $10^{2}$ | 1 | 0.05 (5) | $1.26 \pm 0.23$ | $0.79 \pm 0.18$ |
| | $10^{-2}$ | 1 | 50 (0.5) | $0.95 \pm 0.04$ | $0.92 \pm 0.08$ |

We first ran the experiment at a fixed injection speed with different rate constants, running each simulation to $5t_p$, i.e., until five equivalents of catalyst had been added. Fig. SI4 shows the results for three rate constants spanning four orders of magnitude.

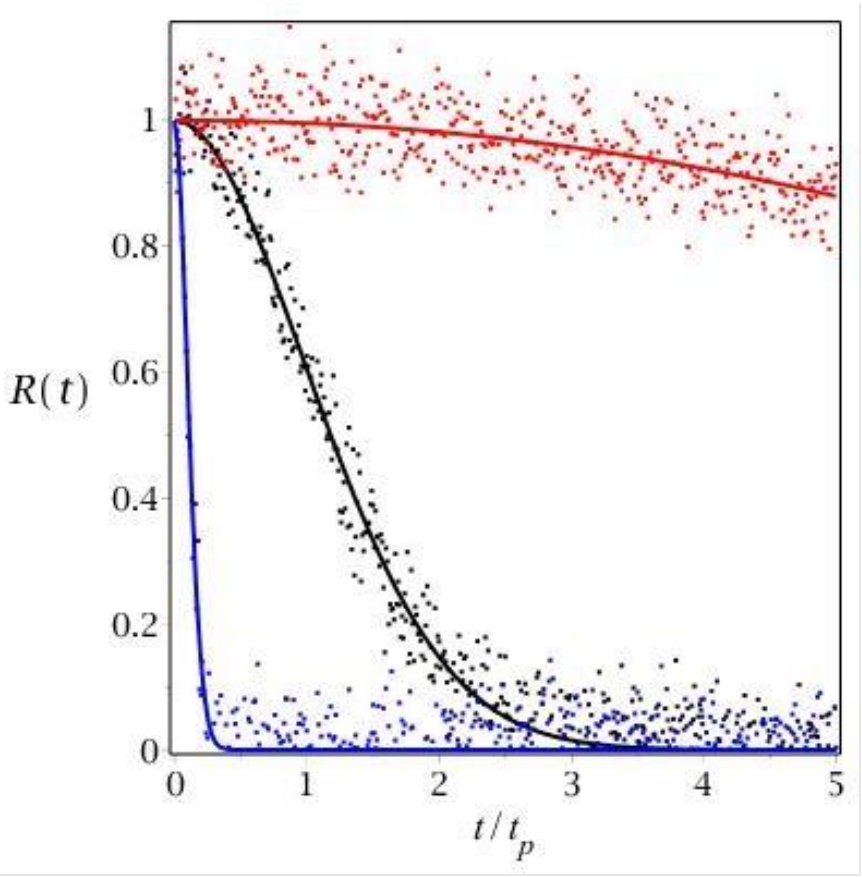


**Fig. SI4** Reactant concentration profiles for three different rate constants. One unit on the time axis corresponds to the time to add one equivalent of catalyst. Simulated data with 5% added normally-distributed noise. Solid lines are the fitted curves: (a) black: $k$ = 1 (true), 0.97±0.01 (fitted); (b) red: $k$ = 0.01 (true), 0.0090±0.0018 (fitted); (c) blue: $k$ = 100 (true), 73±18 (fitted). Errors are standard errors of the fit. Rate constants are in units of $M^{-2}$ $t_p^{-1}$.

The rate constants are reliably found though the accuracy degrades from 2% when the timescales match (black curve, $t_k = 0.69t_p$) to 20% when $t_k$ is 100 times larger or smaller. The remedy for the case where the reaction is much faster than the experimental timescale (blue curve) is to lower the catalyst concentration: injecting 100 times less catalyst in slows the reaction and restores the accuracy of the fit.

For the slow, poorly catalyzed reaction (red curve), it is perhaps surprising that the rate constant (and value of $n$) can be determined so well by fitting only the early part of the overall curve. Increased accuracy can be achieved by running to collect the full curve, but this is expensive of catalyst. For example, 6% accuracy is found when the data is acquired for the time required to inject 30 equivalents of catalyst. An alternative is to better match $t_p$ to $t_k$ by injecting more catalyst: injecting 100 times as much catalyst over the same time period restores the accuracy of fit.

*Simulations with varying number of data points and noise level*

We used simulations to study the effect on the reliability of the fitted values as a function of the number of data points and noise level. The case $m$ = 2, $n$ = 1, $k$ = 1 was investigated in detail, for 20, 50 or 100 data points and normally-distributed random noise with standard deviations of 1%, 2% or 5%. The methods are the same as in the simulations above. The results are summarized in Fig. SI5.

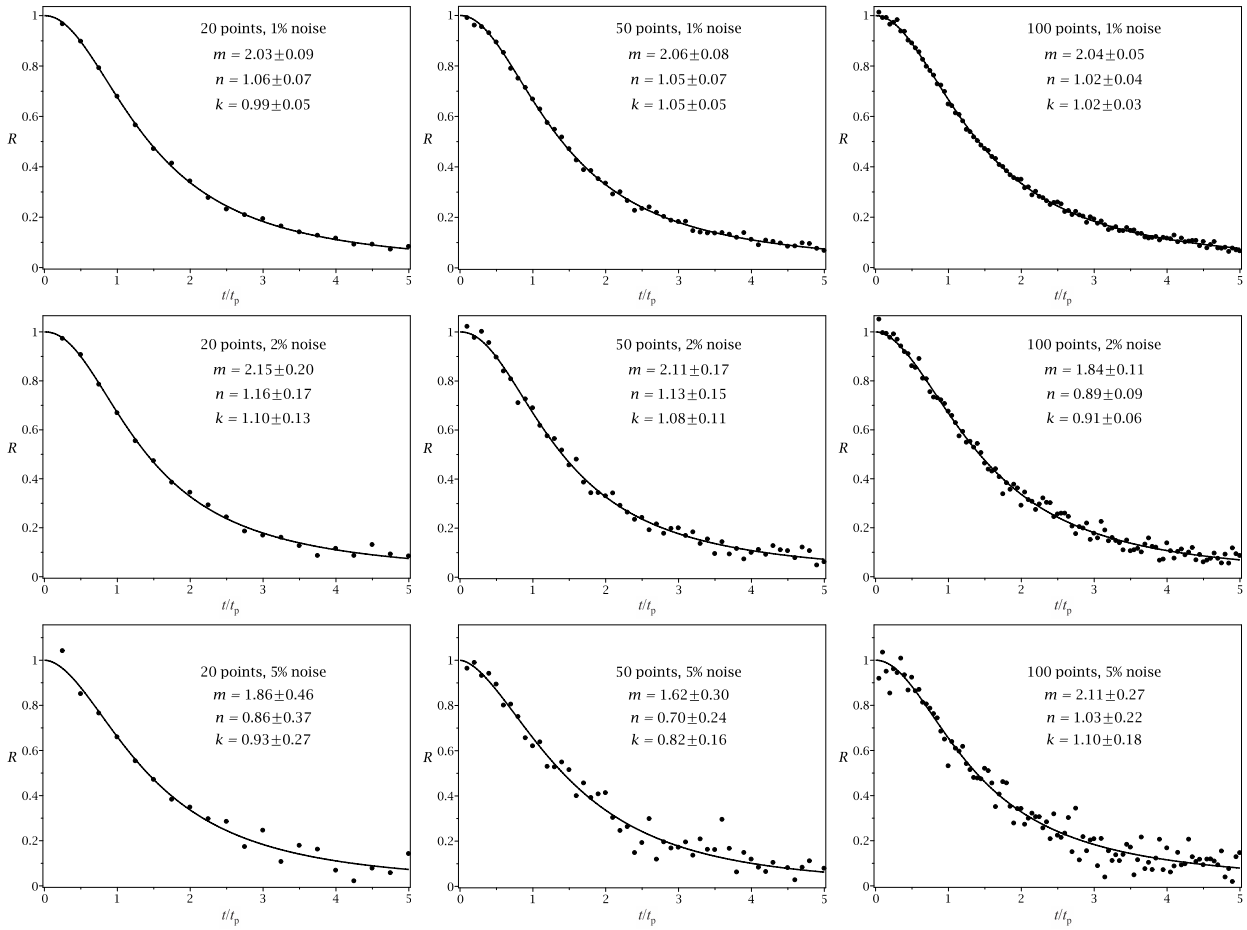


**Fig. SI5** Reactant concentration profiles for different data densities and noise levels. Fits to the *Rmn* equation above with fixed parameters $R_0 = 1$ and $p = 1$. One unit on the time axis corresponds to the time to add one equivalent of catalyst. Solid lines are the fitted curves. The fitted values of $m$, $n$, and $k$ are shown on the plot together with their standard errors, and may be compared to the expected values of $m = 2$, $n = 1$, $k = 1$.

These simulations show standard errors of less than 10% for 1% noise levels, even with only 20 data points. The error in determining the parameters is strongly dependent on the noise level and relatively independent of the number of data points.

## Author contributions

The project was conceptualized by JSM and CK. Formal analysis was performed by PJHW and DAH. Investigations were carried out by PJHW, CK, IC, WM, JS and DK. Methodology was developed by PJHW, CK, IC, WM, JS and JSM. Software was written by PJHW, BH and SD. Supervision by JSM. Validation by PJHW, CK, IC and WM. Visualization by PJHW and BH. Writing by JSM, DAH, PJHW, CK and IC.

## Acknowledgements

We thank NSERC (Discovery and RTI programs) and the University of Victoria for operational and infrastructural support.

## References


1 K. J. Laidler, *Chemical kinetics*, Harper & Row, New York, 3rd ed., 1987.
2 J. I. Steinfeld, J. S. Francisco and W. L. Hase, *Chemical kinetics and dynamics*, Prentice Hall, Upper Saddle River, N.J, 2nd ed., 1999.
3 R. B. Jordan, *Reaction mechanisms of inorganic and organometallic systems*, Oxford University Press, Oxford; New York, 2007.
4 M. Soustelle, *An Introduction to Chemical Kinetics: Soustelle/An Introduction to Chemical Kinetics*, John Wiley & Sons, Inc, Hoboken, NJ, USA, 2011.
5 Y. Ben-Tal, P. J. Boaler, H. J. A. Dale, R. E. Dooley, N. A. Fohn, Y. Gao, A. García-Domínguez, K. M. Grant, A. M. R. Hall, H. L. D. Hayes, M. M. Kucharski, R. Wei and G. C. Lloyd-Jones, *Progress in Nuclear Magnetic Resonance Spectroscopy*, 2022, **129**, 28–106.
6 J. Wang, M. A. Horwitz, A. B. Dürr, F. Ibba, G. Pupo, Y. Gao, P. Ricci, K. E. Christensen, T. P. Pathak, T. D. W. Claridge, G. C. Lloyd-Jones, R. S. Paton and V. Gouverneur, *J. Am. Chem. Soc.*, 2022, **144**, 4572–4584.
7 J. N. Jaworski, C. V. Kozack, S. J. Tereniak, S. M. M. Knapp, C. R. Landis, J. T. Miller and S. S. Stahl, *J. Am. Chem. Soc.*, 2019, **141**, 10462–10474.
8 R. Łobiński and Z. Marczenko, *Critical Reviews in Analytical Chemistry*, 1992, **23**, 55–111.
9 S. L. Younas and J. Streuff, *ACS Catal.*, 2021, **11**, 11451–11458.
10 T. C. Malig, L. P. E. Yunker, S. Steiner and J. E. Hein, *ACS Catal.*, 2020, **10**, 13236–13244.
11 Y. Sato, J. Liu, A. J. Kukor, J. C. Culhane, J. L. Tucker, D. J. Kucera, B. M. Cochran and J. E. Hein, *J. Org. Chem.*, 2021, **86**, 14069–14078.
12 R. G. Belli, Y. Wu, H. Ji, A. Joshi, L. P. E. Yunker, J. S. McIndoe and L. Rosenberg, *Inorg. Chem.*, 2019, **58**, 747–755.
13 L. P. E. Yunker, Z. Ahmadi, J. R. Logan, W. Wu, T. Li, A. Martindale, A. G. Oliver and J. S. McIndoe, *Organometallics*, 2018, **37**, 4297–4308.
14 D. G. Blackmond, *J. Am. Chem. Soc.*, 2015, **137**, 10852–10866.
15 D. G. Blackmond, *Angew. Chem. Int. Ed.*, 2005, **44**, 4302–4320.
16 J. S. Mathew, M. Klussmann, H. Iwamura, F. Valera, A. Futran, E. A. C. Emanuelsson and D. G. Blackmond, *J. Org. Chem.*, 2006, **71**, 4711–4722.
17 J. Burés, *Angew. Chem. Int. Ed.*, 2016, **55**, 16084–16087.
18 A. Martínez-Carrión, M. G. Howlett, C. Alamillo-Ferrer, A. D. Clayton, R. A. Bourne, A. Codina, A. Vidal-Ferran, R. W. Adams and J. Burés, *Angew. Chem. Int. Ed.*, 2019, **58**, 10189–10193.
19 G. López-Cueto and A. F. Cueto-Rejón, *Anal. Chem.*, 1987, **59**, 645–648.
20 M. Márquez, M. Silva and D. Pérez-Bendito, *Analyst*, 1988, **113**, 1733–1736.
21 A. Velasco, M. Silva and D. Pérez-Bendito, *Anal. Chem.*, 1992, **64**, 2359–2365.
22 G. López-Cueto, J. M. Santiago, M. L. Martín-Carratalá, A. F. Cueto-Rejón and N. Grané, *Analytica Chimica Acta*, 1996, **335**, 185–199.
23 O. P. Schmidt and D. G. Blackmond, *ACS Catal.*, 2020, **10**, 8926–8932.
24 H. A. Liebhafsky, *J. Am. Chem. Soc.*, 1932, **54**, 1792–1806.
25 R. Barlag and F. Nyasulu, *J. Chem. Educ.*, 2010, **87**, 78–80.
26 J. C. Hansen, *J. Chem. Educ.*, 1996, **73**, 728.
27 R. S. Livingston and W. C. Bray, *J. Am. Chem. Soc.*, 1923, **45**, 2048–2058.
28 T. Limpanuparb, C. Ruchawapol and D. Sathainthammanee, *J. Chem. Educ.*, 2019, **96**, 812–818.
29 R. H. Crabtree, *Chem. Rev.*, 2015, **115**, 127–150.
30 R. Theron, Y. Wu, L. P. E. Yunker, A. V. Hesketh, I. Pernik, A. S. Weller and J. S. McIndoe, *ACS Catal.*, 2016, **6**, 6911–6917.
31 M. Butters, J. N. Harvey, J. Jover, A. J. J. Lennox, G. C. Lloyd-Jones and P. M. Murray, *Angewandte Chemie International Edition*, 2010, **49**, 5156–5160.
32 C. Amatore, A. Jutand and G. Le Duc, *Chem. Eur. J.*, 2011, **17**, 2492–2503.
33 P. W. N. M. van Leeuwen, *Applied Catalysis A: General*, 2001, **212**, 61–81.

34 S. Erhardt, V. V. Grushin, A. H. Kilpatrick, S. A. Macgregor, W. J. Marshall and D. C. Roe, *J. Am. Chem. Soc.*, 2008, **130**, 4828–4845.
35 S. B. Kedia and M. B. Mitchell, *Org. Process Res. Dev.*, 2009, **13**, 420–428.
36 C. P. Delaney, D. P. Marron, A. S. Shved, R. N. Zare, R. M. Waymouth and S. E. Denmark, *J. Am. Chem. Soc.*, 2022, **144**, 4345–4364.
37 K. Bendinskas, C. DiJiacomo, A. Krill and E. Vitz, *J. Chem. Educ.*, 2005, **82**, 1068.
38 C. L. Copper and E. Koubek, *J. Chem. Educ.*, 1998, **75**, 87.
39 S. W. Wright and Phil Reedy, *J. Chem. Educ.*, 2002, **79**, 41.
40 E. Vitz, *J. Chem. Educ.*, 2007, **84**, 1156.
41 G. T. Thomas, S. Donnecke, I. C. Chagunda and J. S. McIndoe, *Chemistry Methods*, 2022, **2**, e202100068.
42 K. L. Vikse, Z. Ahmadi, C. C. Manning, D. A. Harrington and J. S. McIndoe, *Angew. Chem. Int. Ed.*, 2011, **50**, 8304–8306.
43 S. Aquino Neto, J. C. Forti, V. Zucolotto, P. Ciancaglini and A. R. De Andrade, *Process Biochemistry*, 2011, **46**, 2347–2352.
44 T. P. Silverstein, *J. Chem. Educ.*, 2016, **93**, 963–970.